

## Utilisation of sea nodules leaching residue for adsorption of Ni(II) ions.

N. S. Randhawa<sup>a\*</sup>, Deepak Dwivedi<sup>b</sup>, Sonu Prajapati<sup>b</sup> and R. K. Jana<sup>a</sup>

<sup>a</sup>Metal Extraction & Forming Division, CSIR-National Metallurgical Laboratory, Jamshedpur-831007

<sup>b</sup>Department of Metallurgical and Materials Engineering, O.P. Jindal Institute of Technology,  
Raigarh-496001

\*Corresponding author: N. S. Randhawa, Email: nsr@nmlindia.org

### Abstract

Polymetallic sea nodules may be considered as lean grade ore of Cu, Ni & Co. After recovery of these valuable metals, a huge quantity of residue (~70% of ore body) is generated. In the present paper, investigations carried out for the application of leached sea nodule residue for the removal of Ni(II) from aqueous solution by adsorption, are described. Several parameters have been varied to study the feasibility of using residue as potential adsorbent for remediation Ni(II) contaminated water. The adsorption kinetics followed pseudo first-order equation and the rate of adsorption increased with solution temperature. Kinetics data of Ni(II) adsorption was also discussed using diffusion models of Webber-Morris and Dumwald-Wagner models. The equilibrium data was best fitted into Langmuir adsorption isotherm and the maximum adsorption capacities was found to be 15.15 mg g<sup>-1</sup> at pH 5.5 and temperature 303 K, which decreased to 10.64 mg g<sup>-1</sup> upon raising the solution temperature to 323 K. The activation energy for Ni(II) adsorption onto leached sea nodule residue was 9.56 kJ mol<sup>-1</sup> indicated physical sorption. Desorption studies showed successful regeneration of adsorbent and recovery of Ni. This process can be utilised for removal and recovery of Ni from the industrial effluent.

**Keywords:** Adsorption; Manganese nodule leached residue; Heavy metals; Nickel; Diffusion.

### 1. Introduction

The Pb, Co, Ni, Cu and Zn etc are the common heavy metals found in metal polluted water bodies. The metal finishing and electroplating industries generate considerable amount of effluent containing Pb, Cu, Ni, Co, Zn etc., which contaminate not only the surface water but also the ground water<sup>[1]</sup>. Among these heavy metals, Ni is a toxic heavy metal that is widely used in silver refineries, electroplating, zinc base coating and storage battery industries<sup>[2]</sup>. The chronic toxicity of nickel to human and the environment has been well documented. For example, high concentration of nickel (II) causes cancer of lungs, nose and bone. Soil contamination by Ni has been reported as threat to the crop productivity of the whole world as Ni is readily transported from roots to over ground plant tissue<sup>[3,4]</sup>. Several methods have been developed for remediation of nickel contaminated water bodies such as chemical precipitation, electro-coagulation, ion-exchange etc.<sup>[3,4]</sup> Compared with precipitation and ion exchange treatment, adsorption has been viewed as most versatile and effective method for removing heavy metals from aqueous solutions. Adsorbents based on zeolites, activated carbon etc. have been adequately utilised for adsorptive removal of nickel<sup>[3]</sup>. However, for selection of an adsorbent, cost has been considered prime factor and hence use of low cost adsorbents like activated carbon produced from wastes, clay, biosorbents, fly-ash etc. have also been studied over the years for removal of nickel from contaminated water<sup>[1,4-9]</sup>.

Metallic oxides (Fe, Mn, Al etc.), especially of waste category, are of much interest due to their effectiveness towards adsorptive remediation of heavy metals from contaminated aqueous bodies<sup>[10]</sup>. Residues generated after hydrometallurgical treatment of manganese nodules or polymetallic sea nodules contain oxides/oxy-hydroxides of Fe, Mn, Al and Si with a reasonable porosity and surface area. These residues have been utilized as an effective adsorbent for a variety of species<sup>[11-13]</sup>. In the present work, studies were aimed to investigate the sorption characteristics of residue, generated in the reduction–roast ammoniacal leaching of manganese nodules, for the removal of Ni(II) from its aqueous solution. Several parameters such as adsorbent dose, Ni concentration, pH of solution, temperature and time have been varied to investigate the Ni adsorption characterization of leached sea nodules residue.

## 2. Experimental

### 2.1 Adsorbent

The adsorbent material i.e. leached manganese nodule residue (MNR) was obtained from large scale trial of Reduction roasting - ammoniacal leaching of manganese nodules at CSIR-National Metallurgical Laboratory, Jamshedpur, India. To remove the entrapped leach liquors, MNR was washed with deionised water with 1:10 solid to liquid ratio and stirring for 2 hours. The washed manganese nodule residue (wMNR) was separated by filtration and washed with deionised water followed by air-drying for several days for subsequent characterization and adsorption studies.

### 2.2 Solution preparation

The synthetic stock solution of Ni(II) of 1000 mgL<sup>-1</sup> was prepared by dissolving Ni(NO<sub>3</sub>)<sub>2</sub>·6H<sub>2</sub>O in deionised water and the solution was made slightly acidic by adding a few drops of HNO<sub>3</sub> to prevent hydrolysis of the solution. Solutions of 0.01M HNO<sub>3</sub> and 0.01M NaOH were used for pH adjustment with the help of digital pH meter (Toshniwal CL54) after calibration using NBS buffers. 0.1N KNO<sub>3</sub> was used to maintain the ionic strength in all the adsorption experiments. All the chemicals were Merck-AR grade.

### 2.3 Sample characterisation

For chemical analyses, a weighed quantity of MNR or wMNR was digested in acid (HCl/HNO<sub>3</sub> mixture), dehydrated, redissolved in HCl (1:1) and filtered. The dehydrated silica was estimated gravimetrically while major and minor constituents in the filtrate were analysed by conventional wet chemical methods<sup>[14]</sup> and AAS (Perkin Elmer AAnalyst 400), respectively. Surface area measurements was conducted using Quantachrome 4000E surface area analyser (Nova Instruments, USA). Size analysis was carried out in Malvern Mastersizer after ultrasonic liberation of particles.

### 2.4 Adsorption experiments

For kinetic studies, typically, 100 mL of Ni solution at desired concentration with appropriate amounts of adsorbent was taken in a 250 mL stoppered conical flask. The required pH was adjusted and flask was then mechanically shaken (120 strokes min<sup>-1</sup>) using a water bath shaker, which was maintained at temperatures 303, 313 and 323 K as per requirement. Samples were withdrawn at certain time interval and the solid adsorbent was separated by filtration. The remaining nickel in the filtrate was analyzed by atomic absorption spectrometer (PerkinElmer AAnalyst400). The amount of nickel per gram of the wMNR,  $Q_t$  (mg g<sup>-1</sup>) was calculated using Eq. (1).

$$Q_t = \frac{(C_o - C_t) V}{w \times 1000} \quad (1)$$

Where,  $C_o$  and  $C_i$  are the initial Ni(II) concentration ( $\text{mg L}^{-1}$ ) and Ni (II) in solution respectively, and  $V$  is the volume of solution in mL and  $w$  the mass of sorbent in gram.

The equilibrium adsorption experiments were carried out to investigate the effect of various parameters, such as pH of the adsorbate solution (3-8), initial Ni(II) concentration (5 to 100  $\text{mg L}^{-1}$ ), adsorbent dose (0.25-5.0  $\text{g L}^{-1}$ ) and temperature (303-323 K) under fixed equilibration time obtained by kinetic experiments. For the desorption studies, nickel loaded was transferred into 250mL deionised water adjusted to different pH values in the range of 2 to 9 maintained by 0.1M  $\text{HNO}_3$  and 0.1M  $\text{NaOH}$  and shaken for 2 h at 303 K. The sorbent was filtered and the filtrate was analyzed to determine the concentration of the desorbed metals. Desorption (%) was calculated according to the following equation:

$$\text{Desorption (\%)} = \frac{\text{Amount of metal ion desorbed}}{\text{Amount of metal ions adsorbed}} \times 100 \quad (2)$$

### 3. Results & discussions

#### 3.1 Adsorbent characterisation

Detailed chemical analysis of manganese nodule residue (MNR) and washed residue (wMNR) is given in Table 1. The manganese, iron and silicon are the major constituents along with lime, magnesia and alumina.

**Table 1** Chemical analysis of manganese nodule residue (MNR) and washed residue (wMNR)

| Element/radical         | Chemical composition, % by mass |           |
|-------------------------|---------------------------------|-----------|
|                         | MNR                             | wMNR      |
| Mn                      | 25.66                           | 26.11     |
| Fe                      | 9.92                            | 10.19     |
| $\text{SiO}_2$          | 15.28                           | 16.44     |
| $\text{Al}_2\text{O}_3$ | 3.53                            | 3.54      |
| S                       | 0.37                            | 0.08      |
| $\text{NH}_4^+$         | 0.30                            | Not found |
| Moisture                | 8.96                            | 6.18      |
| $\text{LOI}^b$          | 18.85                           | 17.01     |

After washing, marginal changes in wt% of Mn, Fe,  $\text{SiO}_2$ , C, CaO and MgO but significant loss of S and P is observed. Removals of S and P during washing suggested that part of them are present in soluble form generated from roasting of manganese nodules. Thus washing of MNR was found to be necessary prior to adsorption studies. The  $\text{pH}_{\text{pzc}}$  and specific gravity of wMNR were found to be 6.5 and 3.1, respectively. The BET surface areas of MNR and wMNR are found to be 60.9 and 66.7  $\text{m}^2/\text{g}$ , respectively. The marginally higher surface area of wMNR is presumably due to an increased number of accessible pores on washing out adsorbed species from MNR. Particle size analyses of wMNR revealed very fine granulometry with mean particle diameters ( $d_{50}$ ) of 17.8  $\mu\text{m}$ .

#### 3.2 Effect of pH

The solution pH is an important parameter which affects adsorption of heavy metal ions. The adsorption of nickel was studied over the pH range of ~ 3–8 and the results are shown in Fig. 1. It is seen that the adsorption of Ni(II) increases with increase of pH. Increase in adsorption with pH of

solution may be attributed to competitive binding between  $\text{H}_3\text{O}^+$  ions and  $\text{Ni(II)}$  ions at the  $w\text{MNR}$  surface. As pH value increases, the competing effect of  $\text{H}_3\text{O}^+$  ions decreases and the positively charged  $\text{Ni(II)}$  ions get adhere to free binding sites. The other important factor, which might contribute to the higher adsorption of metal ions with increased pH, is the  $\text{pH}_{\text{pzc}}$  of  $w\text{MNR}$ . When the solution pH exceeded  $\text{pH}_{\text{pzc}}$ , the metal species are more easily attracted by the negatively charged surface of adsorbent, favoring accumulation of metal species on the surface and thus promoting adsorption<sup>[15]</sup>.

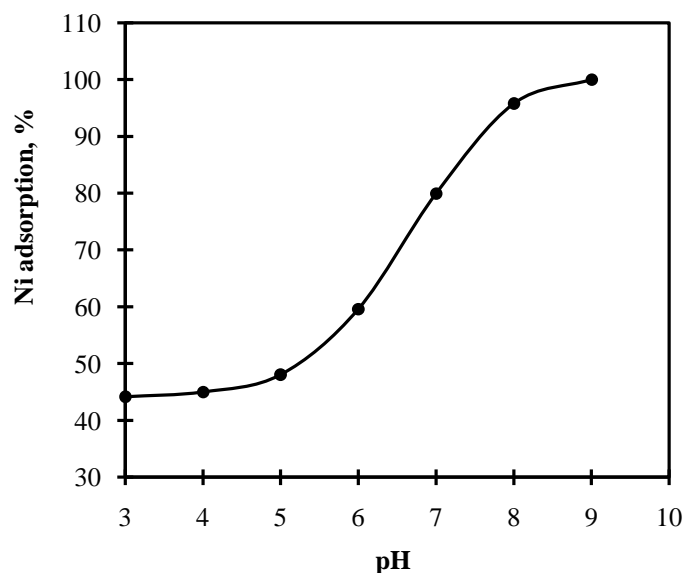


**Fig. 1** Effect of pH on  $\text{Ni(II)}$  adsorption on  $w\text{MNR}$ . Conditions:  $[\text{Ni(II)}]$ ,  $50 \text{ mg L}^{-1}$ ; temperature,  $303 \text{ K}$ ;  $w\text{MNR}$ ,  $1000 \text{ mg L}^{-1}$

### 3.3 Effect of adsorbent dose

Adsorption of  $\text{Ni(II)}$  with varying adsorbent dose, carried out to assess the effect of adsorbent on  $\text{Ni(II)}$  removal, is presented in Fig. 2, where equilibrium  $\text{Ni(II)}$  concentration i.e.  $C_e$  are plotted against  $w\text{MNR}$  dose.

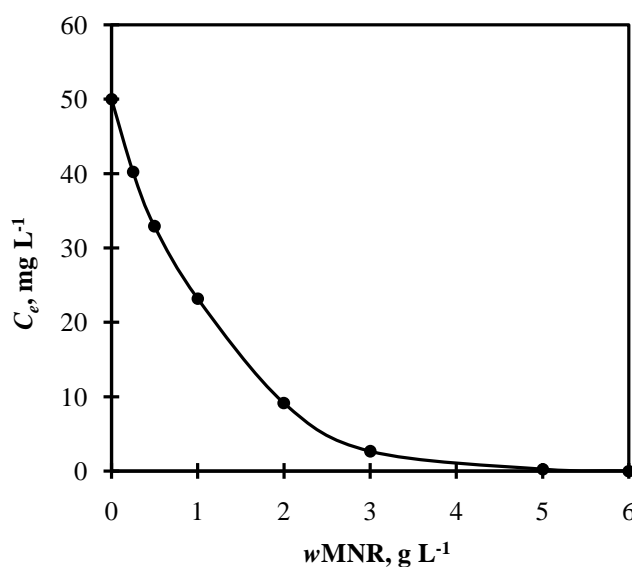


**Fig. 2** Effect of weight of  $w\text{MNR}$  on equilibrium concentration ( $C_e$ ) of  $\text{Ni(II)}$ . Conditions:  $[\text{Ni(II)}]$ ,  $50 \text{ mg L}^{-1}$ ; temperature,  $303 \text{ K}$ ; time,  $2 \text{ h}$ ;  $\text{pH } 5.5$

The results show that the equilibrium concentration ( $C_e$ ) of Ni(II) decreases with increase in the weight of wMNR, which is  $40 \text{ mg L}^{-1}$  for  $0.25 \text{ g Ni L}^{-1}$  wMNR and negligible for  $5.0 \text{ g L}^{-1}$  of wMNR addition. Increase of wMNR dose provides higher surface area and active sites for adsorption of Ni(II) and ultimately responsible for more uptake of Ni(II).

### 3.4 Effect of time and initial concentration on adsorption

The time course of Ni(II) adsorption onto wMNR at varying initial concentrations is given in Fig. 3. The Ni(II) adsorption increase with time and attains equilibrium at  $\sim 120 \text{ min}$  irrespective of initial concentration of Ni(II) ions. Similar equilibrium time has been reported for Ni(II) adsorption onto turkish flyash<sup>[9]</sup>, however, numbers of systems are reported to have equilibrium achieved between 15 min to 1hr<sup>[15-20]</sup>. On the other hand, higher equilibrium adsorption times of about 4 hrs are reported for chitin<sup>[19]</sup> and pine tree material<sup>[20]</sup> based adsorbents. The amount of adsorption is found to decrease with the increasing initial Ni(II) concentration. The Ni(II) removal at equilibrium is 43, 21, 12 and 11 % for 25, 50, 75 and  $100 \text{ mg L}^{-1}$  initial Ni(II), respectively. For a fixed dose of adsorbent the decrease in adsorption with increasing Ni(II) concentration is primarily due to availability of limited number of site for adsorption. However, uptake of Ni(II) onto wMNR is seen to be markedly increased.

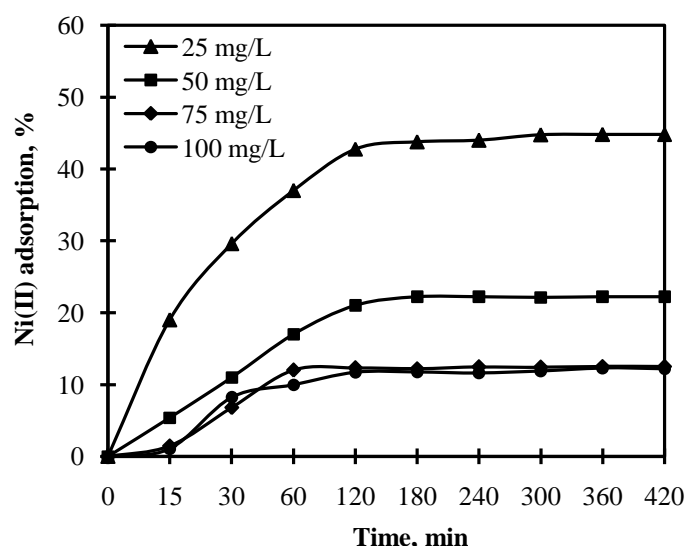


**Fig. 3** Effect of time and initial concentration on Ni(II) adsorption onto wMNR. Conditions: pH, 5.5 , Temperature, 303K, wMNR,  $1000 \text{ mg L}^{-1}$

### 3.5 Adsorption kinetics

The adsorption data obtained from time variation studies was fitted into reaction based as well as diffusion based models (given in Table 2) to investigate the kinetics of Ni(II) adsorption by wMNR. The kinetics data was fitted into these models and interestingly, all the four plots obtained were almost linear (figure not shown). The corresponding rate constants and correlation coefficient values calculated from slope and intercept of the kinetic plots are given in Table 3. On the basis of regression coefficient values, it is concluded that Ni(II) sorption onto wMNR can be approximated more appropriately by the pseudo first-order kinetic model than the second-order kinetic model. Higher regression coefficient values obtained from webber-morris and Dumwald-Wagner model (Table 3) also indicated possible role of diffusion within particles during Ni(II) sorption. In addition,

slope in the intraparticle diffusion given by Webber and Morris was found to start from origin and hence, it should be considered rate limiting step<sup>[21]</sup>.

**Table 2** Kinetic models for adsorption rate calculations<sup>[22-25]</sup>.

| Kinetic models       |                                                         | Plot                    | Slope           | Intercept             |
|----------------------|---------------------------------------------------------|-------------------------|-----------------|-----------------------|
| 1. Reaction based    |                                                         |                         |                 |                       |
| Pseudo first-order   | $\ln(q_e - q_t) = \ln q_e - k_1 t$                      | $\ln(q_e - q_t)$ Vs $t$ | $k_1$           | $\ln q_e$             |
| Pseudo second-order  | $\frac{t}{q_t} = \frac{1}{k_2 q_e^2} + \frac{1}{q_e} t$ | $t/q_t$ Vs $1/t$        | $\frac{1}{q_e}$ | $\frac{1}{k_2 q_e^2}$ |
| 2. Diffusion based   |                                                         |                         |                 |                       |
| Weber-Morris model   | $q_t = k_{id} \cdot t^{1/2} + I$                        | $q_t$ Vs $t^{1/2}$      | $k_{id}$        | $I$                   |
| Dumwald-Wagner model | $\log(1 - F^2) = - \frac{kt}{2.303}$                    | $\log(1 - F^2)$ Vs $t$  | $k$             |                       |

**Table 3** kinetic model rate constants for Ni(II) adsorption on wMNR at different temperatures.

| Temperature (K) | <i>Pseudo first-order model</i>                 |                             |                                               |       |
|-----------------|-------------------------------------------------|-----------------------------|-----------------------------------------------|-------|
|                 | $k_1$ (min <sup>-1</sup> )                      | $q_e$ (mg g <sup>-1</sup> ) | $r^2$                                         |       |
| 303             | 0.0284                                          | 0.999                       | 9.64                                          |       |
| 313             | 0.0331                                          | 0.999                       | 7.38                                          |       |
| 323             | 0.0359                                          | 0.998                       | 6.29                                          |       |
|                 | <i>Pseudo second-order model</i>                |                             |                                               |       |
|                 | $k_2$ (g mg <sup>-1</sup> min <sup>-1</sup> )   | $q_e$ (mg g <sup>-1</sup> ) | $V_o$ (mg g <sup>-1</sup> min <sup>-1</sup> ) | $r^2$ |
| 303             | 0.004                                           | 0.998                       | 12.165                                        | 0.563 |
| 313             | 0.005                                           | 0.995                       | 7.886                                         | 0.310 |
| 323             | 0.005                                           | 0.986                       | 5.882                                         | 0.174 |
|                 | <i>Webber-Morris model</i>                      |                             |                                               |       |
|                 | $K_{id}$ (mg g <sup>-1</sup> h <sup>0.5</sup> ) | Intercept, C                | $r^2$                                         |       |
| 303             | 9.268                                           | 0.265                       | 0.993                                         |       |
| 313             | 5.945                                           | -0.004                      | 0.998                                         |       |
| 323             | 4.284                                           | -0.153                      | 0.998                                         |       |
|                 | <i>Dumwald-Wagner model</i>                     |                             |                                               |       |
|                 | $K$                                             | $r^2$                       |                                               |       |
| 303             | -0.010                                          | 0.993                       |                                               |       |
| 313             | -0.012                                          | 0.993                       |                                               |       |
| 323             | -0.013                                          | 0.989                       |                                               |       |

The kinetics of the Ni(II) adsorption found to be improved by increasing temperature from 303K to 323K as evident from increased rate constant for pseudo first-order model (Table 3) though equilibrium Ni(II) uptake was adversely affected, presumably an indication of physisorption<sup>[21]</sup>. Another evidence in support of physical sorption of Ni(II) onto wMNR was obtained when activation energy of Ni(II) adsorption was calculated using following expression.

$$k_1 = k.e^{\left(-\frac{E_a}{RT}\right)} \quad (3)$$

where,  $k_i$  is the rate constant for pseudo first-order kinetics ( $\text{g mg}^{-1}\text{min}^{-1}$ ),  $k$  is the temperature-independent factor ( $\text{g mg}^{-1}\text{min}^{-1}$ ),  $E_a$  the activation energy of sorption ( $\text{kJ mol}^{-1}$ ),  $R$  the universal gas constant ( $8.314 \text{ J mol}^{-1} \text{ K}$ ) and  $T$  the solution temperature ( $\text{K}$ ). The activation energy of Ni(II) adsorption onto wMNR was calculated from the slope of straight line obtained by plot between  $\ln k_i$  versus  $1/T$ . The magnitude of the activation energy is commonly used as the basis for differentiating between physical and chemical adsorption. The activation energy for Ni(II) adsorption onto wMNR was found to be  $9.56 \text{ kJ mol}^{-1}$  for  $25 \text{ mgL}^{-1}$  initial concentrations, confirmed that the Ni(II) ions are physically adsorbed onto the wMNR surface<sup>[21]</sup>.

### 3.6 Adsorption isotherms

The equilibrium adsorption data were fitted into the linearized form of isotherm models proposed by Langmuir (Eq. 4) and Freundlich (Eq. 5) models<sup>[13]</sup>.

$$\frac{C_e}{q_e} = \frac{1}{bQ^o} + \frac{C_e}{Q^o} \quad (4)$$

$$\ln q_e = (1/n) \ln C_e + \ln K_f \quad (5)$$

where,  $C_e$  is equilibrium concentration ( $\text{mg L}^{-1}$ );  $q_e$  is amount adsorbed at equilibrium ( $\text{mg g}^{-1}$ );  $b$  is Langmuir isotherm constants related to affinity of adsorbent toward metal ion and  $Q^o$  is adsorption maxima or adsorption capacity ( $\text{mg g}^{-1}$ ). The  $K_f$  and  $1/n$  stand for empirical constants related to adsorption capacity and intensity, respectively. The calculated parameter from Langmuir plot of  $C_e$  versus  $C_e/q_e$  and Freundlich plot of  $\ln q_e$  versus  $\ln C_e$  are given in Table 4.

**Table 4** Langmuir and Freundlich isotherm model parameters and coefficients for adsorption of Ni(II) on wMNR.

| Temp,<br>K | Langmuir isotherm               |                                             |       | Freundlich isotherm             |       |       |
|------------|---------------------------------|---------------------------------------------|-------|---------------------------------|-------|-------|
|            | $Q_o$<br>( $\text{mg g}^{-1}$ ) | $b$<br>( $\text{mg L}^{-1}$ ) <sup>-1</sup> | $R^2$ | $K_f$<br>( $\text{mg g}^{-1}$ ) | $1/n$ | $R^2$ |
| 303        | 15.15                           | 0.16                                        | 0.994 | 3.48                            | 0.34  | 0.914 |
| 313        | 13.33                           | 0.08                                        | 0.993 | 2.06                            | 0.41  | 0.952 |
| 323        | 10.64                           | 0.09                                        | 0.996 | 1.78                            | 0.35  | 0.937 |

The Langmuir model is more likely applicable due to higher correlation coefficients, suggesting possible monolayer coverage of Ni(II) on the surface of wMNR. Further, the value of  $Q^o$ , which is a measure of adsorption capacity, decreased with the rise in temperature. This is also supported by the findings from kinetic studies, where uptake of Ni(II) showed decrease with temperature (Table 3). Dimensionless separation factor,  $R_L$ , measure of favorability of adsorption, was calculated using Eq. (6).

$$R_L = \frac{1}{1 + bC_o} \quad (6)$$

Where,  $C_o$  is the initial metal concentration ( $\text{mg L}^{-1}$ ) and  $b$  is the Langmuir parameter i.e. energy of interaction at the surface. The conditions,  $R_L > 1$ : unfavorable;  $R_L = 1$ : linear;  $0 < R_L < 1$ : favourable;  $R_L = 0$ : irreversible, are reported in literature<sup>[3]</sup>. The calculated value of  $R_L$  was obtained in the range 0.098-0.553, suggesting that the adsorption of Ni(II) on wMNR is favorable and reversible.

### 3.7 Release of metal ions

Release of metal ions from leached residue during Ni(II) adsorption was also investigated to understand its behavior at different pH. Fig. 4 shows that some amount of metal ions, especially Mn ions, leached out into adsorbate solution. The release of Cu, Co and Fe is, however, not included in the figure, as their release was negligibly small and detectable only at pH <3. It may be noted that the release of  $\text{Mn}^{2+}$  was significantly lowered with increasing solution pH. The other metal ions released were Ca and Mg only, which were decreased with increasing pH and were negligibly small at pH ~ 5-6. These values are well within the permissible limit set by WHO for different metal ions in drinking water.

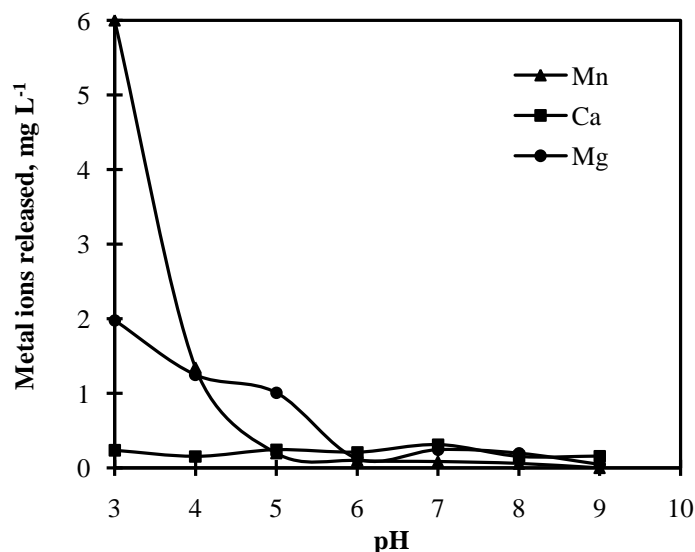


**Fig. 4** Release of different metal ions during adsorption of Ni(II) at varying pH. [Ni(II)], 50 mg L<sup>-1</sup>; temperature, 303 K; wMNR, 1000 mg L<sup>-1</sup>; Time, 60 min.

### 3.8 Loading capacity

The  $Q^o$  i.e. maximum loading capacity value for Ni adsorption on this adsorbent as determined by Langmuir isotherm data was found to be 15.15 mg g<sup>-1</sup> at 303 K (Table 4). The temperature adversely affected the uptake of  $\text{Ni}^{2+}$  onto wMNR decreasing loading capacity to 13.33 mg g<sup>-1</sup> at 313 K and further down to 10.64 mg g<sup>-1</sup> at 323 K. A comparative account of the adsorption capacities of some adsorbents and wMNR for removal of  $\text{Ni}^{2+}$  are given in Table 5.

**Table 5** Comparative adsorption capacity of some adsorbents for Ni(II) ions in aqueous solution.

| Adsorbents                      | pH  | Initial metal ion concentration, mg L <sup>-1</sup> | Adsorption capacity, mg g <sup>-1</sup> | Reference    |
|---------------------------------|-----|-----------------------------------------------------|-----------------------------------------|--------------|
| Amino Phosphate chelating resin | -   | -                                                   | 5.39                                    | [26]         |
| Natural coated sand             | 7   | 30-110                                              | 1.08                                    | [15]         |
| Almond husk (Activated carbon)  | 5   | 25-250                                              | 30.769                                  | [16]         |
| Paper mill sludge               | 4.5 | 5-100                                               | 7.861                                   | [17]         |
| Modified pine bark              | 8   | 1-100                                               | 20.58                                   | [20]         |
| Modified pine cone              | 8   | 1-100                                               | 1.67                                    | [20]         |
| Clinoptilolite                  | 6.2 | 10-800                                              | 15.55                                   | [27]         |
| Fly ash                         | 6   | -                                                   | 2.89                                    | [4]          |
| wMNR                            | 5.5 | 5-100                                               | 15.15                                   | Present work |



The wMNR has loading capacity almost equal to clinoptilolite but significantly higher nickel than that for most of the adsorbents listed in Table 5 except activated carbon produced from almond husk and the modified pine bark. Thus, wMNR can be effectively utilised as potential adsorbent for Ni(II) removal from contaminated water.

### 3.9 Desorption studies

Since the adsorption of Ni(II) is strongly dependent on pH of the solution, its desorption from wMNR can be effected by controlling the pH of the eluent. The desorption of Ni(II) from nickel loaded wMNR was carried out under varying pH and results obtained are presented in Fig. 5. It is seen that ~ 98 % of the adsorbed nickel is desorbed at pH  $\approx$  2 and thereafter, the desorption of Ni(II) progressively decreases with increasing pH of the eluent. This indicates that Ni(II) adsorption on wMNR is completely reversible and the Ni(II) ions that are physically adsorbed through electrostatic attraction can be desorbed.

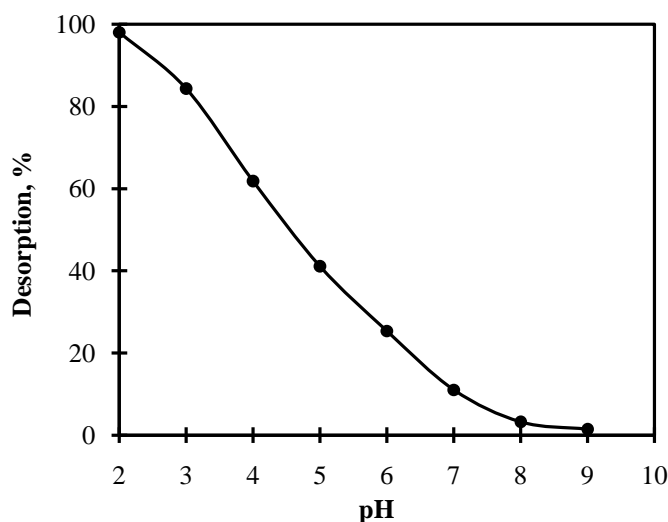


**Fig. 5** Desorption of loaded Ni<sup>2+</sup> ions from wMNR at varying pH.

### 4. Conclusion

The use of residue, from reduction roasting –ammonia leaching of manganese nodule, for the adsorption of Ni(II) from aqueous solution has been examined. The percentage removal of Ni(II) depends on the initial Ni(II) ions concentration and decreases with increase in initial Ni concentration. The adsorption was fairly rapid and equilibrium was achieved within 4 h contact time. The adsorption capacity increases with increasing pH. The percentage removal of Ni(II) increases rapidly with increase in the dose adsorbent due to the increase in the surface area of the adsorbent. The decrease in the equilibrium adsorption of Ni(II) with increasing temperature indicates the Ni(II) ions removal by adsorption on leached sea nodule residue is exothermic in nature. Langmuir isotherm shows better fit to adsorption data than the Freundlich model indicating monolayer sorption of Ni(II) onto wMNR. The monolayer loading capacity of 15.15 mg g<sup>-1</sup> was obtained at 303 K, which decreased to 13.33 mg g<sup>-1</sup> at 313 K and down to 10.64 mg g<sup>-1</sup> at 323 K. The experimental data were fitted by the pseudo first order kinetic model. The intraparticle diffusion given by Webber and Morris was found to be rate limiting step with slope starting from origin.

## 5. Acknowledgement

The authors wish to thank the Director, CSIR-NML, Jamshedpur for his permission to publish this paper. Two of authors, Deepak Dwivedi and Sonu Parajapati, show their gratitude to the Director, CSIR-NML for his kind permission to carry out training work at CSIR-NML, Jamshedpur.

## 6. References

- [1] Hussein, A.I., Mamdouh, F.A., Raouf, A.O., 1998, *Environ. Manage. Health.* 9, p. 170.
- [2] Bhattacharya, A.K., Naiya, T.K., Mandal, S.N., Das, S.K., 2008, *Chem. Eng. J.* 137, p. 529.
- [3] Zheng, W., Zhang, L.S., Jing, Q.Z., 2009, In: *Proc. 3rd International Conference on Bioinformatics and Biomedical Engineering (ICBBE-2009)*, Nanjing, China p. 1.
- [4] Jadia, C.D., Fulekar, M.H., 2009, *African J. Biotech.* 8, p. 921.
- [5] Wang, S., Ming, H.T., Slo, M.T., 2008, *Bioresource Technol.* 99, p. 7027.
- [6] Belgin, B., 2002, *J. Hazard. Mater.* 95, p. 251.
- [7] Paul, D.J., Mermoz, S., Emmanuel, D., Pascal, K., Daniel, N., 2012, *J. Applied Surf. Sci.*, 258, p. 7470.
- [8] Moodley, K., Singh, R., Musapatika, T.E., Maurice, O.S., Ochieng, A., 2011, *Water SA* 37, p. 41
- [9] Bayat, B., 2002, *J. Hazard. Mater.* B95, p. 251.
- [10] Lee, G.F., 1974, *Proc. of Symposium of Transport of Heavy Metals in the Environment*, IN: *Progress in Water Technology* 17, p. 137.
- [11] Jana, R.K., Pandey, B.D., Premchand, 1999, *Hydrometallurgy* 53, p. 45.
- [12] Jana, R.K., Srikanth, S., Pandey, B.D., Kumar, V., Premchand, 1999, *Met. Mater. Proc.* 11, p. 133.
- [13] Das, N.N., Jana, R.K., 2006, *J. Colloid Interf. Sci.* 293, p. 253.
- [14] Vogel, A.I., 1978, In: *A text book of quantitative inorganic analysis*, 4<sup>th</sup> Edn. (Longmans, London) p. 375; 373; 242.
- [15] Boujelben, N., Bouzid, J., Elouear, Z., 2009, *J. Hazard. Mater.* 163, p. 376.
- [16] Hasar, H., *J. Hazard. Mater.* B97, p. 49.
- [17] Suryan, S., Ahluwalia, S.S., 2012, *Inter. J. Environ. Sci.* 2, p. 1331.
- [18] Green-Pederson, H., Jensen, B.T., Pind, N., 1997, *J. Environ. Technol.* 18, p. 807.
- [19] Hema, S., Kumuran, T.M., Sudha, P.N., 2011, *Inter. J. Environ. Sci.* 2, p. 624.
- [20] Argun, M.E., Dursun, S., Gur, K., Ozdemir, C., Karatas, M., Dogan, S., 2010, *J. Environ. Technol.* 26, p. 479.
- [21] Srivastava, V.C., Mall, I.D., Mishra, I.M., 2006, *J. Hazard. Mater.* 134, p. 257.
- [22] Lagergren, S., *Kungliga Svenska Vetenskapsakademien. Handlingar* 24, p. 1.
- [23] Ho, Y.S., 2004, *Scientometrics* 59, p. 171.
- [24] Ho, Y.S., McKay, G., 1998, *Proc. Safety Environ. Protection* 76, p. 332.
- [25] Ho, Y.S., 2006, *J. Hazard. Mater.* 136, p. 103.
- [26] Meng, F.W., 2005, MS Thesis, Nanjing University, China, p. 28.
- [27] Sprzynski, M., Buszewski, B., Terzyk, A. P., Namiesnik, J., 2006, *J. Colloid. Interf. Sci.* 304, p. 21.